Independent Speed Control of Two Parallel Connected Split-Phase IM With a Common DC Link and Inverter

Sagar Kumar Dash, *Student Member, IEEE*, and R. Sudharshan Kaarthik, *Member, IEEE*

***Abstract*—A novel pulsewidth modulation (PWM) scheme for the decoupled and coordinated control of two parallel connected split-phase induction machines is discussed in this paper for the first time. Both the motors are operated from a single six-phase voltage source inverter which acts as a power source, and two switched capacitor-fed auxiliary inverters to limit the flow of non-torque producing currents in each motor. Both the motors can be operated at its full rated power with low switching frequency, and decoupled control for full power range can be achieved with the proposed topology. This is possible because the individual machines do not carry the load/harmonic currents of other machine (unlike the conventional series or parallel connected systems). The converters can be modulated using sine-triangle PWM or space vector pulsewidth modulation (SVPWM). Furthermore, two different schemes of SVPWM techniques are proposed and compared in this paper. Exhaustive experimental results for all the modulation schemes are provided for steady state and transient operating conditions including start-up to validate the proposed topology and modulation schemes.**

***Index Terms*—Capacitor-fed inverter, decoupled control, split-phase induction motors (IM), sinusoidal pulsewidth modulation (SPWM), space vector PWM (SVPWM), voltage source inverter (VSI).**

I. Introduction

NUMEROUS applications utilize multimotor drive systems such as electric vehicles, more-electric aircrafts, ship propulsion, winders, and locomotives. Three-phase motor drives are predominantly used for most of the existing multidrive system, where each machine is supplied from its own voltage source inverter (VSI) with appropriate independent control algorithms. Achieving independent flux and torque control, and operating multiple three-phase machines with full power, while being fed from a single three-phase VSI is not possible. However, the decoupled control of machines can be achieved in a multimotor multiphase machine drive system. Furthermore, multiphase machines possess certain advantages compared to their three-phase counterpart such as higher torque density, greater efficiency, reduced torque pulsations, reduced stress in semiconductor switches, improved noise characteristics of the drive, greater fault tolerance, and increase in reliability [1], [2].

Manuscript received September 24, 2018; revised November 28, 2018; accepted January 13, 2019. Date of publication January 23, 2019; date of current version June 28, 2019. Recommended for publication by Associate Editor D. G. Xu. *(Corresponding author: R. Sudharshan Kaarthik.)*

S. Kumar Dash is with the Department of Electrical Engineering, Indian Institute of Technology Kharagpur, Kharagpur 721302, India (e-mail:

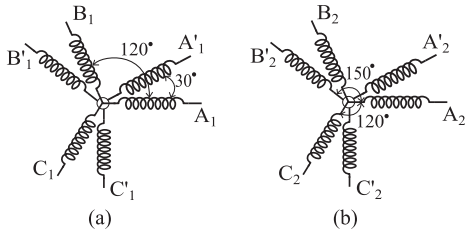

Fig. 1. (a) Stator winding of split-phase motor (M1). (b) Reconfigured stator winding of split-phase motor (M2).

A split-phase (asymmetric six-phase) machine is a multiphase motor having six phases on the stator, achieved by splitting the phase belt of a conventional three-phase motor winding into two equal halves with phase separation of 30 electrical degrees between the two windings [3] as shown in Fig. 1(a). This asymmetrical configuration has the following advantages. 1) For the same air-gap flux, the inverter dc-link voltage requirement is reduced to nearly half, i.e., $V_{\rm dc}/(2\cos 15^\circ)$, where $V_{\rm dc}$ is the dc-link voltage of the VSI used for the three-phase machine. 2) Harmonic cancellation occurs due to the mutual cancellation of the air-gap flux for all the $6n \pm 1$ ($n =$ odd) harmonic voltages, which results in complete elimination of sixth harmonic torque pulsations in the split-phase arrangement. A split-phase (double star) induction machine drive supplied from a six-phase inverter was first proposed in [4] and [5]. Due to the harmonic flux cancellation, and the absence of back EMF for opposing these harmonic voltages, the usage of VSI for driving split-phase motor drives resulted in high $6n \pm 1$ ($n =$ odd) stator harmonic currents [6]. These harmonic currents should be suppressed by bulky and expensive harmonic filters [7], or using capacitor-fed auxiliary inverters with high-frequency switching [8]. An efficient PWM technique for split-phase induction motor (IM) is described in [9].

The control scheme of a multiphase machine drive (no of phases $\geqslant 5$) utilizes only fundamental field component for the torque production, so it requires only two stator current components (i.e., α–β current components). The remaining degrees of freedom (i.e., z_1–z_2 current components) can be utilized in a

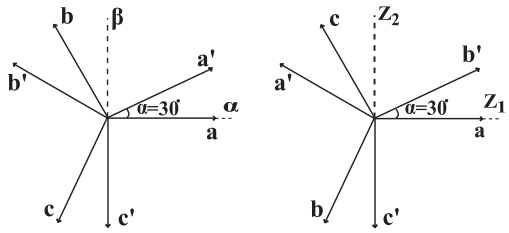

Fig. 2. Voltage vectors in α–β and z_1–z_2 plane.

different manner [10], in this case to drive another motor, which is the basis for multimotor multiphase drive systems [11].

The Cartesian vector approach to reference frame theory for ac machines is discussed in [12], and it further extended for multiphase machines in [13]. The vector space decomposition technique can be used to analyze the six-phase machines as discussed in [6]. For the split-phase machine M1 [see Fig. 1(a)], the harmonic voltage components are decomposed into three sets of orthogonal planes

$$\begin{aligned}&\begin{bmatrix} V_\alpha & V_\beta & V_{z1} & V_{z2} & V_{O1} & V_{O2}\end{bmatrix}'\\ &= [C]\begin{bmatrix} V_a & V_{a'} & V_b & V_{b'} & V_c & V_{c'}\end{bmatrix}'\\ &[C] = \end{aligned} \tag{1}$$

$$\sqrt{\frac{1}{3}}\begin{bmatrix} 1 & \cos(\alpha) & \cos(4\alpha) & \cos(5\alpha) & \cos(8\alpha) & \cos(9\alpha)\\ 0 & \sin(\alpha) & \sin(4\alpha) & \sin(5\alpha) & \sin(8\alpha) & \sin(9\alpha)\\ 1 & \cos(5\alpha) & \cos(8\alpha) & \cos(\alpha) & \cos(4\alpha) & \cos(9\alpha)\\ 0 & \sin(5\alpha) & \sin(8\alpha) & \sin(\alpha) & \sin(4\alpha) & \sin(9\alpha)\\ 1 & 0 & 1 & 0 & 1 & 0\\ 0 & 1 & 0 & 1 & 0 & 1\end{bmatrix}$$

where $\alpha = \pi/6$. $V_a, V_{a'}, V_b, V_{b'}, V_c, V_{c'}$ are the motor's phase voltages. V_α and V_β are the two orthogonal voltage components, belonging to $6n \pm 1$ ($n =$ even) harmonic voltages including the fundamental component spans the α–β plane, which contribute toward the air-gap flux, and electromagnetic torque in M1. V_{z1} and V_{z2} are the two orthogonal voltage components of $6n \pm 1$ ($n =$ odd) harmonics spanning the z_1–z_2 plane, which does not contribute to the flux/torque production due to harmonic cancellation of flux in the air gap. V_{01} and V_{02} are the zero-sequence voltage components of triple harmonics set spanning the O_1–O_2 plane, which does not produce currents because of the double-star connected (isolated) neutrals. Fig. 2 shows the stator voltages spanning α–β and z_1–z_2 plane. By using the transformation matrix (1), all harmonic voltage components of the respective six-phase machines can be decomposed into their respective orthogonal planes, which allows independent control of both motors M1 and M2.

II. Operating Principle of Two Parallel Connected Split-Phase IM

The principle of decoupled and independent control of two split-phase IMs connected in parallel while being fed from a single VSI lies in the fact that the torque producing component (α–β current) of machine M1 [see Fig. 1(a)] is not producing torque in M2. Similarly, the torque producing component (z_1–z_2 current) of machine M2 [see Fig. 1(b)] is not producing torque in M1. This is achieved by adopting proper phase transposition of stator windings of multiphase machines. The independent field-oriented control of series-connected split-phase machines is discussed in [14] and [15]. The stator winding connection schemes for even-phase series connected multimotor vector controlled drive with a single inverter supply is discussed in [16]. In [17], the modeling and control of two five-phase series connected drive system was discussed. A five-phase parallel-connected multiphase machine supplied from a single VSI was attempted and reported in [18].

In the proposed topology, two phase transposed motors (M1 and M2) are connected in parallel, power being supplied to both motors by a single VSI. The main VSI is modulated with the sum of voltages required by motors M1 and M2. In addition to the load current, the motor M1 draws large harmonic currents due to the presence of V_{z1z2}, and similarly, motor M2 draws large harmonic currents due to the presence of $V_{\alpha\beta}$. To limit these unwanted harmonic currents, two auxiliary (AUX) VSIs are connected at the other ends of the motors (open-end configuration) and these inverters act as switched capacitive filters as shown in Fig. 3. The AUX VSI-1 supplies z_1–z_2 voltages and AUX VSI-2 supplies α–β voltages to this proposed scheme as explained in Sections III-A and III-B. The modulating voltages for the main VSI are as follows:

$$[v_{\text{main}}] = \frac{[C]^{-1}}{V_{\text{DC}}}\begin{bmatrix} V_\alpha & V_\beta & V_{z1} & V_{z2} & V_{O1} & V_{O2}\end{bmatrix}' \tag{2}$$

where $[v_{\text{main}}]$ is the modulating voltage for each inverter leg of the main VSI. The modulating voltages for AUX VSI-1 $[v_{\text{AUX VSI-1}}]$ and AUX VSI-2 $[v_{\text{AUX VSI-2}}]$ are as follows:

$$[v_{\text{AUX VSI-1}}] = \frac{2[C]^{-1}}{V_{\text{DC}}}\begin{bmatrix} 0 & 0 & V_{z1} & V_{z2} & 0 & 0\end{bmatrix}' \tag{3}$$

$$[v_{\text{AUX VSI-2}}] = \frac{2[C]^{-1}}{V_{\text{DC}}}\begin{bmatrix} V_\alpha & V_\beta & 0 & 0 & 0 & 0\end{bmatrix}'. \tag{4}$$

The proposed parallel connected scheme for decoupled control of two split-phase IMs for the full power range operation can be used to overcome the issues and difficulties of the previously mentioned series and parallel connected systems, which are discussed as follows.

1) The main VSI can operate with low switching frequency, which minimizes the switching losses hence suitable for high-power drive applications.
2) The unwanted harmonic current components (i.e., z_1–z_2 currents for M1 and α–β currents for M2) are totally eliminated by using capacitor-fed auxiliary inverters.
3) The power rating of main inverter is the sum of the power ratings of both the motors. While the power ratings of the auxiliary VSIs are a fraction of the main inverter's power rating and depend on the modulation scheme.
4) Both machines can operate at its full rated power simultaneously as they do not carry the harmonic currents (and the load current of other machine) as in the case of series connected system, and the unwanted harmonic currents in the case of parallel connected system of [18].
5) Voltage stress on the phase windings of machines is reduced because of the use of auxiliary VSIs.

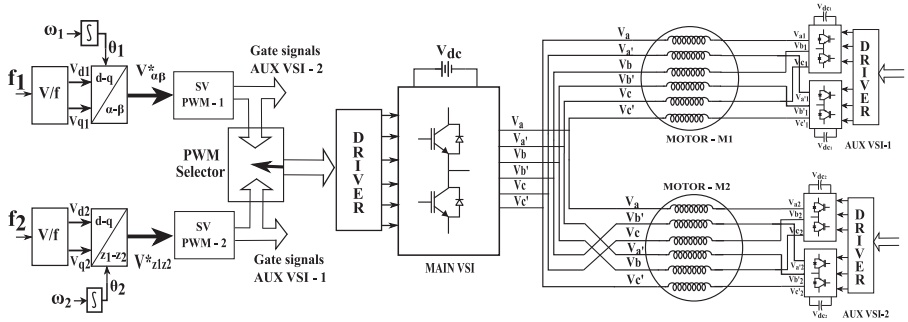

Fig. 3. Space vector PWM implementation for independent control of two split-phase IMs using split dc-link capacitive filter.

6) This topology does not require any additional power sources, precharging circuits. The dc-link capacitors of auxiliary VSIs have inherent charge balancing capability.
7) The proposed scheme has reduced number (36) of semiconductor switches compared to conventional switched capacitor filter-based topologies for split-phase machines (48 required) [8].

A. Power Contribution From Auxiliary Inverters

The AUX VSI-1 (see Fig. 3) is modulated with z_1–z_2 voltages, i.e., the phase sequence of voltage is: $v_a - v_{b'} - v_c - v_{a'} - v_b - v_{c'}$, while the phase sequence of currents drawn by M1 is: $i_a - i_{a'} - i_b - i_{b'} - i_c - i_{c'}$. Therefore, the instantaneous power input $p(t)$ to the AUX VSI-1 is

$$\begin{aligned} p(t) &= (v_a i_a + v_{a'} i_{a'} + v_b i_b + v_{b'} i_{b'} + v_c i_c + v_{c'} i_{c'}) \\ &= V_m I_m [(\sin(\omega t)\sin(\omega t - \phi)) \\ &\quad + \sin(\omega t - 150^\circ)\sin(\omega t - \phi - 30^\circ) \\ &\quad + \sin(\omega t - 240^\circ)\sin(\omega t - \phi - 120^\circ) \\ &\quad + \sin(\omega t - 30^\circ)\sin(\omega t - \phi - 150^\circ) \\ &\quad + \sin(\omega t - 120^\circ)\sin(\omega t - \phi - 240^\circ) \\ &\quad + \sin(\omega t - 270^\circ)\sin(\omega t - \phi - 270^\circ)] \end{aligned} \tag{5}$$

where V_m and I_m are the peak value of the phase voltage and current, respectively, ω is the angular frequency and t is the time, ϕ is the phase angle between motor phase voltage and current. Average power input P_{avg} to the AUX VSI-1 is

$$\begin{aligned} P_{\text{avg}} &= \frac{1}{2\pi}\int_0^{2\pi} p(t)\, d(\omega t) \\ &= \frac{V_m I_m}{2\pi}[\pi\cos(\phi) + \pi\cos(120^\circ - \phi) \\ &\quad + \pi\cos(120^\circ - \phi) + \pi\cos(120^\circ + \phi) \\ &\quad + \pi\cos(120^\circ + \phi) + \pi\cos(\phi)] \end{aligned} \tag{6}$$

$$= 0. \tag{7}$$

Hence from the power requirement criteria, the dc-link current can be calculated from power balance as follows:

$$\begin{aligned} P_{\text{avg}} &= V_{\text{dc1}} I_{\text{dc1}} = 0; V_{\text{dc1}} \neq 0 \\ &\Rightarrow I_{\text{dc1(avg)}} = 0. \end{aligned} \tag{8}$$

Similarly, AUX VSI-2 is modulated with α–β voltages, with the phase sequence $V_a - V_{a'} - V_b - V_{b'} - V_c - V_{c'}$ and the fundamental phase currents drawn by the motor M2 flows through the AUX VSI-2. The phase sequence of the motor M2 currents is $I_a - I_{b'} - I_c - I_{a'} - I_b - I_{c'}$. The average power input to the AUX VSI-2 can be calculated in the similar manner as discussed

$$\begin{aligned} p(t) &= (v_a i_a + v_{a'} i_{a'} + v_b i_b + v_{b'} i_{b'} + v_c i_c + v_{c'} i_{c'}) \\ P_{\text{avg}} &= \frac{1}{2\pi}\int_0^{2\pi} p(t)\, d(\omega t) = 0 \\ P_{\text{avg}} &= V_{\text{dc2}} I_{\text{dc2}} = 0; V_{\text{dc2}} \neq 0 \\ &\Rightarrow I_{\text{dc2(avg)}} = 0. \end{aligned} \tag{9}$$

As the average dc currents (I_{dc1} and I_{dc2}) through the auxiliary dc-link sources are zero, the auxiliary VSIs do not source or sink any active power. These sources are replaced with capacitors as shown in Fig. 3. Precharging of capacitors is not required as they are charged through their respective stator winding currents of the motors. Furthermore, the proposed topology provides an inherent dc-link balancing capability for the AUX VSIs. The dc-link voltages remain stable during all the operating conditions like steady state, transients, and disturbances, which are experimentally verified and shown in Section IV.

B. Sizing of Main and Auxiliary Inverters

The main inverter supplies the current required by both the motors (i.e., sum of the currents of M1 and M2) to drive them. Thus, the main inverter is rated to supply the power consumed by both the motors and the power lost in the AUX INVs.

The auxiliary inverter's dc link depends on its modulation indices. By choosing different modulation schemes, the dc link of the AUX VSIs can be varied. The dc link of AUX VSIs should be sized such that it suppresses the harmonic voltages as well as the current ripple through the IMs. In case of sine triangle PWM scheme, the modulation index of the AUX VSIs is doubled, while that of MAIN VSI is kept unchanged. In case of space vector PWM, the switching time can vary over a period T_s to change the effective modulation index of the AUX VSIs, while that of MAIN VSI is kept unchanged over that period. The AUX VSIs carries the individual motor's current by suppressing the flow of other motor current through it.

For these VSIs operated with sinusoidal pulsewidth modulation (SPWM) scheme, the peak value of output inverter voltages

are given as follows:

$$V_{m_1} = \frac{m_1 V_{\mathrm{dc1}}}{2\cos 15^\circ}; V_{m_2} = \frac{m_2 V_{\mathrm{dc2}}}{2\cos 15^\circ}; V_m = \frac{m V_{\mathrm{dc}}}{2\cos 15^\circ}$$
$$\frac{V_m}{V_{\mathrm{dc}}} = \frac{m_1 + m_2}{2\cos 15^\circ} = \frac{V_{m_1}}{V_{\mathrm{dc}_1}} + \frac{V_{m_2}}{V_{\mathrm{dc}_2}} \tag{10}$$

where m, m_1, and m_2 are the modulation indices, V_m, V_{m_1}, and V_{m_2} are the peak of the output voltages, $V_{\mathrm{dc}}, V_{\mathrm{dc1}}$, and V_{dc2} are the dc-link voltages of MAIN VSI, AUX VSI-1, and AUX VSI-2, respectively, and $m = m_1 + m_2$. Two cases are considered below to derive the dc-link voltage requirement for the AUX VSIs.

1) Case-1 (When Only One Motor Operates): As M1 is modulated with $V_{\alpha\beta}$ and $V_{z_1 z_2} = 0$. For maximum inverter output voltage, the modulation indices are normalized to their maximum value. The AUX VSI-1 is modulated by $V_{z_1 z_2}$, which is zero so the output voltage is $V_{m_1} = 0$. The AUX VSI-2 modulated by $V_{\alpha\beta}$ has the output voltage V_{m_2}. The main VSI has to modulate with $V_{\alpha\beta}$ while keeping $V_{z_1 z_2} = 0$. Hence the output voltage of main VSI and AUX VSI-2 is the same, so the voltage across M2 is zero and it will not produce torque

$$V_m = V_{m_2} \Rightarrow m V_{\mathrm{dc}} = m_2 V_{\mathrm{dc2}}$$
$$V_{\mathrm{dc}_2} = (m/m_2) \times V_{\mathrm{dc}} \tag{11}$$

$$V_m = V_{m_1} \Rightarrow m V_{\mathrm{dc}} = m_1 V_{\mathrm{dc1}}$$
$$V_{\mathrm{dc}_1} = (m/m_1) \times V_{\mathrm{dc}}. \tag{12}$$

2) Case-2 (When Both M1 and M2 Operate): When both the motors are operated with their respective auxiliary inverters and the VSIs are operating at their maximum modulation index, the dc-link voltage requirement can be calculated based on (10). Furthermore, if the modulation indices to the AUX VSIs are given as twice as that of the MAIN VSI, then the dc-link voltage of auxiliary VSIs is half of the dc link of MAIN VSI, i.e.,

$$m_1 = m_2 = 2m$$
$$\text{then, } V_{\mathrm{dc1}} = V_{\mathrm{dc2}} = V_{\mathrm{dc}}/2. \tag{13}$$

On the other hand, if the modulation indices of all the VSIs are kept equal, then the dc link of AUX VSIs is the same as that of MAIN VSI, i.e.,

$$m_1 = m_2 = m$$
$$\text{then, } V_{\mathrm{dc1}} = V_{\mathrm{dc2}} = V_{\mathrm{dc}}. \tag{14}$$

The current flows through the auxiliary inverters are half of the MAIN VSI, and the dc-link voltage depends on the ratio of the modulation indices as shown in (11) and (12). Hence, the power ratings of the auxiliary VSIs are a fraction of the MAIN VSI power depending on the modulation indices.

III. Operation of Dual Split-Phase Drives Using Different PWM Techniques

Improper modulation of VSIs to drive split-phase IM leads to flow of unwanted harmonic currents. Due to sixth-order harmonic-flux cancellation in the stator, excessive harmonic currents flow through the machine causing excessive copper loss. By using proper PWM techniques for the AUX VSIs, the amplitude of the unwanted harmonic currents can be suppressed. In the case when the stator windings are connected with isolated neutrals (see Fig. 3), the currents produced due to the zero-sequence voltages $V_{0_1-0_2}$ is inherently zero, and PWM is performed with constraints only on the α–β and z_1–z_2 planes [3], [4], [6].

A. Sine Triangle PWM for Proposed Parallel Connected Dual Split-Phase Drive

When a split-phase induction motor is fed from a six-phase inverter with sine triangle PWM scheme, the modulating voltages for the six-phase inverter are generated with a time displacement of 30° between two sets of three-phase voltages. By applying the inverse Clarke's transformation $[C]^{-1}$, the reference voltages for the six phases can be obtained

$$\begin{bmatrix} V_{am} & V_{a'm} & V_{bm} & V_{b'm} & V_{cm} & V_{c'm} \end{bmatrix}'$$
$$= [C]^{-1} \begin{bmatrix} V_\alpha^* & V_\beta^* & V_{z1}^* & V_{z2}^* & V_{01}^* & V_{02}^* \end{bmatrix}' \tag{15}$$

where $V_{am}, V_{a'm}, V_{bm}, V_{b'm}, V_{cm}, V_{c'm}$ are the modulating voltages for the six-phase VSI. Let the voltage applied by main VSI be represented as $[V_\alpha, V_\beta, V_{z1}, V_{z2}]$ in α–β and z_1–z_2 planes. Motor-M1 operates in α–β plane, hence V_{z1} and V_{z2} should average out to zero for every sampling interval. This can be achieved by modulating the AUX VSI-1 such that it nullifies or opposes V_{z1} and V_{z2} generated by the main VSI, and ensures the flow of only $I_{\alpha\beta}$ currents which is the torque/flux producing current for M1. Similarly, V_α and V_β should average out to zero for motor-M2 so that it consumes only z_1–z_2 currents. This can be achieved by modulating the AUX VSI-2 such that it nullifies V_α and V_β generated by the main VSI. It restricts the flow of $I_{\alpha\beta}$ current through M2 and ensures the flow of only $I_{z_1 z_2}$ current, which is the torque/flux producing current for M2. Detail explanation is provided in [19].

To implement the SPWM scheme, three sets of modulating signals have to be generated for the three inverters. The modulating voltages for the AUX VSI-1 are generated from $[c]^{-1}$ with the reference voltage of $V_{z_1 z_2}$, while keeping $V_\alpha = V_\beta = 0$. Similarly, the modulating voltages for the AUX VSI-2 are generated from $[C]^{-1}$ with the reference voltage of $V_{\alpha\beta}$, while keeping $V_{z_1} = V_{z_2} = 0$. The MAIN VSI is modulated with both $V_{\alpha\beta}$ and $V_{z_1 z_2}$ reference voltages as shown in Fig. 4. The modulating voltages are given in (2) and (4).

B. Proposed SVPWM for Parallel Connected Dual Split-Phase Drive

For a six-phase motor, the conventional SVPWM technique based on vector space decomposition is proposed in [6]. In a six-phase two-level inverter, $2^6 = 64$ different voltage vectors can be applied to the machine. The goal of SVPWM is to synthesize the four active voltage vectors and one zero vector during each sampling period T_s to generate α–β voltage components to satisfy the torque/flux requirements, and at the same time to maintain the average volt-sec on the z_1–z_2 plane to be zero. The detailed analysis is given in [20].

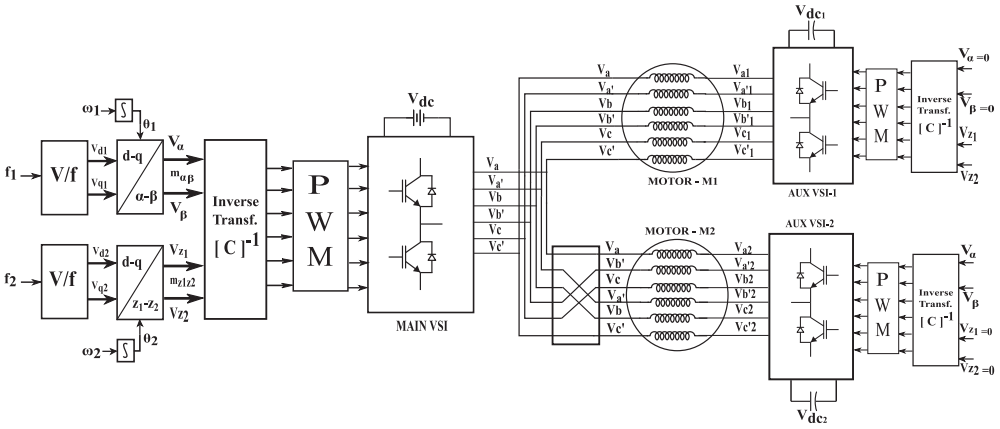

Fig. 4. Sine triangle PWM fed dual split-phase drives with independent control.

1) Dwell Time Calculation: During each sampling period T_s, four active vectors (V1, V2, V3, V4) and one zero vector (V0) are chosen as explained in [6]. This guarantees that the dwell time for each space vector is positive and a unique solution exists, which also results in minimum current harmonics. Only the large vectors are used to synthesize the reference voltage in α–β plane that results in the smallest voltage vectors in z_1–z_2 plane, producing lower current harmonics. The SVPWM is done by calculating the timings for each vector as follows:

$$\begin{bmatrix} T_1 \\ T_2 \\ T_3 \\ T_4 \\ T_0 \end{bmatrix} = \begin{bmatrix} V_\alpha^1 & V_\alpha^2 & V_\alpha^3 & V_\alpha^4 & 0 \\ V_\beta^1 & V_\beta^2 & V_\beta^3 & V_\beta^4 & 0 \\ V_{z_1}^1 & V_{z_1}^2 & V_{z_1}^3 & V_{z_1}^4 & 0 \\ V_{z_2}^1 & V_{z_2}^2 & V_{z_2}^3 & V_{z_2}^4 & 0 \\ 1 & 1 & 1 & 1 & 1 \end{bmatrix}^{-1} \begin{bmatrix} V_\alpha^* \\ V_\beta^* \\ V_{z1}^* \\ V_{z2}^* \\ 1 \end{bmatrix} * T_s \quad (16)$$

where V_m^n is the projection of the nth voltage vector on the m-axis and T_n is the dwell time of that vector during a switching time interval T_s.

The space vector PWM for a five-phase VSI supplying two five-phase series-connected machines is discussed in [21]. Similarly, the two-motor drive system as shown in Fig. 3 has two independent SVPWM modulators. SVPWM-1 generates voltages only in α–β plane and is used to control M1 while the SVPWM-2 generates voltages only in z_1–z_2 plane and is used to control M2.

Four large vectors are chosen to synthesize the reference voltages ($V_{\alpha\beta}^*$ and $V_{z_1 z_2}^*$) from α–β and z_1–z_2 planes [6], respectively. The gating signals generated by SVPWM-1 modulator are given to AUX VSI-2, hence it generates exact $V_{\alpha\beta}$ voltage to suppress the flow of $I_{\alpha\beta}$ through M2. Similarly, the gating signals generated by SVPWM-2 modulator are given to AUX VSI-1, hence it generates exact $V_{z_1 z_2}$ voltage to suppress the flow of $I_{z_1 z_2}$ through M1.

The prime requirement of the space vector modulators is to synthesize both $V_{\alpha\beta}^*$ and $V_{z_1 z_2}^*$ (flux and torque producing voltage components of M1 and M2, respectively) to maintain the average volt-seconds on both α–β and z_1–z_2 reference plane and it has to satisfy the flux/torque requirements of both machines to achieve complete decoupled control [11]. To achieve this requirement, two types of space vector modulation schemes are adopted here.

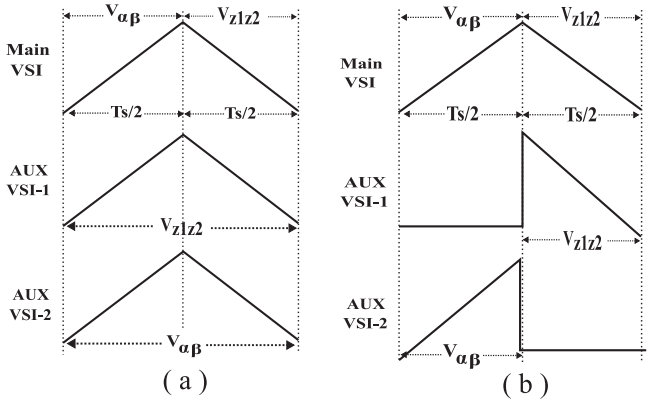

Fig. 5. PWM carrier waveform for MAIN and AUX VSIs for full switching period. (a) Switching scheme-1. (b) Switching scheme-2.

2) SVPWM Scheme - 1: For a sampling period of T_s, in the first half (0 to $T_s/2$), the main VSI applies the torque and flux producing voltages $V_{\alpha\beta}$ for M1, by selecting a set of four active vectors and one zero vector from α–β plane. The selection of the vectors is such that $V_{z_1 z_2}$ for M1 is averaged out to zero in that switching interval, hence no z_1–z_2 harmonic currents flow through M1. For the second half of switching period ($T_s/2$ to T_s), the main VSI applies the torque and flux producing voltages ($V_{z_1 z_2}$) for M2 by selecting a set of four active vectors and one zero vector from z_1–z_2 plane. The selection of the vectors is such that $V_{\alpha\beta}$ is averaged out to zero for the switching duration, so no α–β harmonic currents flow through M2.

The gating signals for the MAIN VSI are generated by the PWM selector (a multiplexer) as shown in Fig. 3. Simultaneously, the AUX VSI-1 is modulated with $V_{z_1 z_2}$ voltages and AUX VSI-2 is modulated with $V_{\alpha\beta}$ voltages throughout the switching period T_s. The effective time of the applied voltage vector is halved for the MAIN VSI, whereas the voltages are not multiplexed for the AUX VSIs during each sampling time, hence the dc-link requirement of AUX VSIs is $V_{\rm dc}/2$. It is the same case as explained in (13). The switching scheme is shown in Fig. 5(a).

3) SVPWM Scheme - 2: In SVPWM scheme-2, the main VSI switching remains exactly the same as that of scheme-1. However, the switching of AUX VSIs is different. During the switching period (0 to T_s/2), the main inverter applies $V_{\alpha\beta}$ voltages to drive M1, the AUX VSI-1 applies zero vector, while AUX VSI-2 applies $V_{\alpha\beta}$ voltage to instantaneously oppose the voltage across the M2 windings. Hence the voltage across M1 windings is $V_{\alpha\beta}$ while voltage across M2 is zero, so, $I_{\alpha\beta}$ flows through M1 and there is no power supplied to M2 during the first half of the switching interval. During $T_s/2$ to T_s main inverter applies $V_{z_1 z_2}$ voltages to drive M2, which is instantaneously opposed by AUX VSI-1 so that there is no voltage across M1. Thus, $I_{z_1 z_2}$ flows through M2 and there is no power supplied to M1 during the second half of the switching interval.

This means that the effective duration of the applied voltages ($V_{\alpha\beta}$ and $V_{z_1 z_2}$) is halved for all the VSIs (main and AUX VSIs). In order to obtain the same average magnitude of the output voltage, the dc-link requirement of AUX VSIs should be the same as that of the main VSI, i.e., $V_{\rm dc}$, as explained in (14). The switching scheme is shown in Fig. 5(b). This scheme reduces the ripple in the phase currents due to instantaneous space vector voltage cancellation, making the current waveforms smoother.

IV. Experimental Results

Two 10-hp, 415-V, 50-Hz, four-pole split-phase induction motors with open-end winding configuration were used for the experiment. The split-phase configuration is derived from a three-phase machine by reconfiguring and splitting the three phases into six-phase asymmetrical winding structure. The motor-M1 is connected as the same winding sequence to the MAIN VSI, while motor-M2 is reconfigured in a different winding sequence as shown in Fig. 1(b). 75-A, 1200-V insulated-gate bipolar transistor (IGBT) half-bridge modules (SKM75GB12T4) were used to realize the switches of the VSIs. A six-phase two-level inverter with a common dc link is used as a main VSI and acts as a power source. It provides the necessary voltages and currents to drive both the motors and connected at the common end of the parallel connected winding configuration. The dc power of the main VSI is derived from a three-phase diode bridge rectifier module with a dc-link capacitor as shown in Fig. 6(b). Two six-phase two-level inverters split into three-phase VSIs with capacitor fed dc link is used as auxiliary inverters, which are connected at the other end of the split-phase IM. The dc link of AUX VSIs uses capacitors, as these inverters do not consume/supply any active power.

The PWM gating signals for all the 36 IGBT switches were generated by a SPARTAN-3 FPGA board at a switching frequency of 2 kHz and the control/modulation schemes were implemented on TMS320F28335 DSP board as shown in the experimental setup [see Fig. 6(a)]. The experimental results of various steady-state operating conditions for scheme-1 and scheme-2 along with some transient results for acceleration and start-up are shown below.

A. Steady-State Results

The steady-state waveforms of the proposed drive scheme are presented in Figs. 7 and 8. Fig. 7 shows the phase current of motors M1 and M2, MAIN VSI, and dc link of AUX VSI for scheme-1. In Fig. 7(a), it shows that M1 is running at 600 r/min while M2 is standstill. The phase-a current of M1 is at 30 Hz while M2 has nearly zero current. The MAIN VSI current is the same as M1 current at this condition.

Fig. 7(b) shows all the current waveforms at 20 Hz when both M1 and M2 operate at the same speed of 600 r/min. Fig. 7(c) shows the current waveforms when both the motors are operating at different speeds (phase current of M1 has 20-Hz component and M2 has 40-Hz component). It can be seen that the MAIN VSI current has both the frequency components of M1 and M2 currents.

Fig. 8 shows the waveforms for different operating conditions of scheme-2. Fig. 8(a) shows phase current of M1 at 30 Hz and M2 has zero currents with negligible switching ripples compared to scheme-1. Fig. 8(b) shows the waveforms for the same speed of operation of M1 and M2 at phase currents of 40 Hz. Fig. 8(c) shows the different speed of operation of M1 and M2 (phase current of M1 has 30-Hz component and M2 has 40-Hz component).

In both cases, three different steady-state operating conditions are considered, single motor operation and dual motor with the same and different speed of operations. It can be observed that the individual motor currents are sinusoidal and carries the current of single-frequency component while that of MAIN VSI will have both the frequency components of M1 and M2. From the motor currents, it can be observed that during steady-state operation they are independent and decoupled from one another. The dc-link voltage of auxiliary VSIs remains stable for all the operating conditions. Furthermore, the current ripple is lower in scheme-2.

B. Transient Results

Different transient conditions are considered such as acceleration of one motor while keeping the other standstill, and constant speed operation, simultaneous acceleration of both motors, transients during stat-ups and operation of motors with and without switching of AUX VSIs.

Fig. 9(a) shows the speeds of M1 and M2, where M1 is accelerated from 300 to 1200 r/min in 5 s while M2 is standstill. Fig. 9(b.1) and (b.2) shows that the phase current envelope of M1 increases during acceleration, and that of M2 remains zero. The MAIN VSI current is exactly the same as that of M1 current as shown in Fig. 9(b.4). Fig. 10(a) shows the speed of M1 is increased from 300 to 1200 r/min in 5 s with a constant acceleration while the speed of M2 is maintained constant at 900 r/min. Fig. 10(b.1) and (b.2) shows that the phase current envelope of M1 increases during acceleration, and that of M2 remains constant during acceleration. The MAIN VSI current is the sum of M1 and M2 currents as shown in Fig. 10(b.4).

Fig. 11(a) shows that both the motors are accelerated simultaneously from 300 to 1200 r/min in 5 s at a constant rate. Fig. 11(b.1) and (b.2) shows the current magnitude and fre-

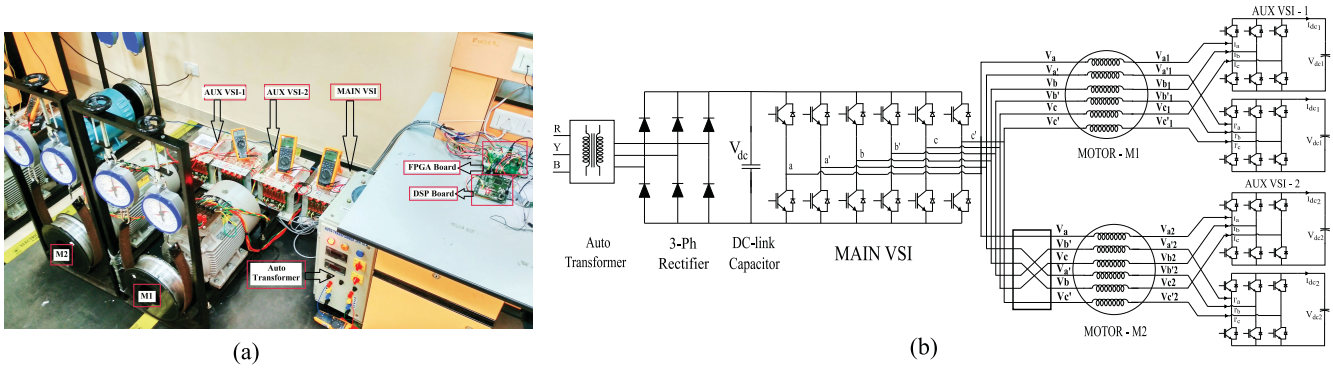

Fig. 6. (a) Photograph of the experimental setup. (b) Experimental circuit diagram of the proposed topology.

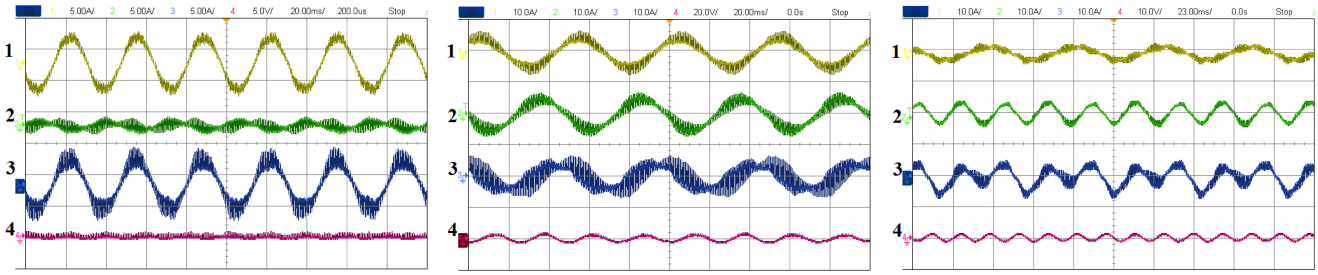

(a) [X-axis:20ms/div; Y-axis:5A/div, 5V/div] (b) [X-axis:20ms/div; Y-axis:10A/div, 20V/div] (c) [X-axis:23ms/div; Y-axis:10A/div, 10V/div]

Fig. 7. Steady-state results for Scheme-1. (a) M1 runs at 900 r/min (30 Hz) and M2 is standstill. (b) Both the motors run at 600 r/min (20 Hz). (c) M1 runs at 600 r/min (20 Hz) and M2 at 1200 r/min (40 Hz). (1) Phase-a current of M1. (2) Phase-a current of M2. (3) Phase-a current of main VSI (M1+M2). (4) DC-link ripple of AUX VSI-1 (V_{dc1}).

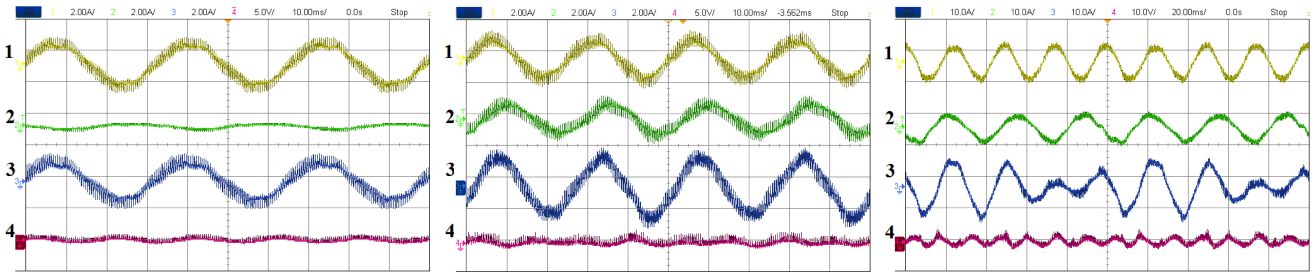

(a) [X-axis:10ms/div; Y-axis:2A/div, 5V/div] (b) [X-axis:10ms/div; Y-axis:2A/div, 5V/div] (c) [X-axis:20ms/div;Y-axis:10A/div, 10V/div]

Fig. 8. Steady-state results for Scheme-2. (a) M1 runs at 900 r/min (30 Hz) and M2 is standstill. (b) Both the motors run at 1200 r/min (40 Hz). (c) M1 runs at 900 r/min (30 Hz) and M2 at 1200 r/min (40 Hz). (1) Phase-a current of M1. (2) Phase-a current of M2. (3) Phase-a current of main VSI (M1+M2). (4) DC-link ripple of AUX VSI-1 (V_{dc1}).

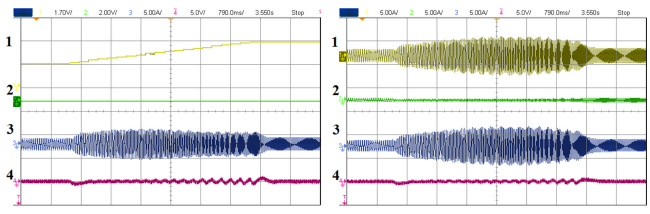

(a) (b)

Fig. 9. Transient results: M1 is accelerating and M2 is standstill. (a).1. Speed of M1: from 300 to 1200 r/min at 5 s; (a).2. Speed of M2: 0 r/min; (b).1. Phase-a current envelope of M1. (b).2. Phase-a current envelope of M2. (3) Phase-a current envelope of main VSI (M1 + M2). (4) Constant dc-link ripple of AUX VSI-1 (V_{dc1}). [X-axis: 790 ms/div; Y-axis: 5 A/div, 5 V/div].

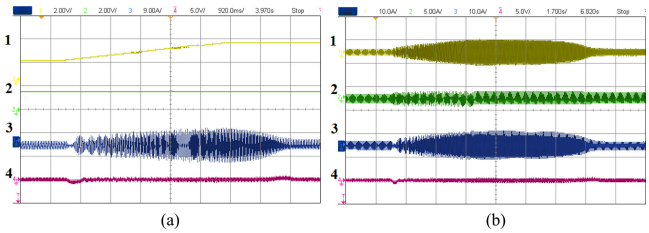

(a) (b)

Fig. 10. Transient results: M1 is accelerating and M2 is at constant speed. (a).1. Speed of M1: from 300 to 1200 r/min at 5 s. (a).2. Speed of M2: fixed at 600 r/min. (b).1. Phase-a current envelope of M1. (b).2. Phase-a current envelope of M2. (3) Phase-a current envelope of main VSI (M1 + M2). (4) Constant dc-link ripple of AUX VSI-1 (V_{dc1}). [X-axis: 920 ms/div; Y-axis: 9 A/div, 5 V/div].

quency of M1 and M2 currents start increasing according to the speed references during acceleration and finally settles during constant speed operation. It can be observed that the amplitude of phase current increases during the acceleration period and settles down to the original value once the speed stabilizes. The motor current waveforms show that the speed of the M2 is

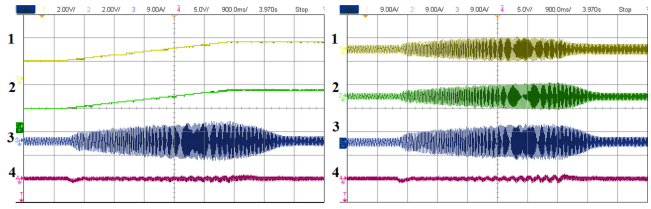

(a) (b)

Fig. 11. Transient results: Simultaneous acceleration of both M1 and M2. (a).1. Speed of M1: from 300 to 1200 r/min at 5 s. (a).2. Speed of M2: from 300 to 1200 r/min at 5 s. (b).1. Phase-a current envelope of M1. (b).2. Phase-a current envelope of M2. (3) Phase-a current envelope of main VSI (M1 + M2). (4) Constant dc-link ripple of AUX VSI-1 (V_{dc1}). [X-axis: 900 ms/div; Y-axis: 9 A/div, 5 V/div].

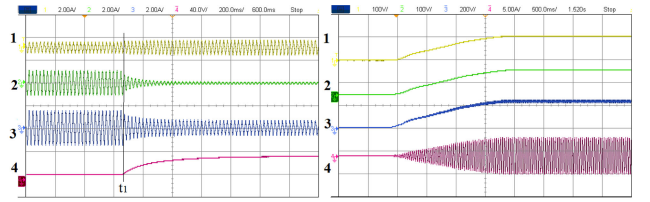

(a) [X-axis: 200ms/div; Yaxis: 2A/div, 40V/div] (b) [X-axis: 500ms/div; Yaxis: 5A/div]

Fig. 12. Transient results: Transients due to AUX VSI switchings and during starting. (a).1. Phase-a current of M1 at 30 Hz. (a).2. Phase-a current of M2 at standstill condition with and without AUX VSI-2. (a).3. Phase-a current envelope of main VSI (M1 + M2). (a).4. Charging of dc-link voltage of AUX VSI-2 from 9 V to steady state. (b).1,2. DC-link voltage of AUX VSI-1 and 2 (100 V/div) during startup. (b).3. DC-link voltage of MAIN VSI (200 V/div). (b).4. Phase-a current envelope of main VSI (M1 + M2).

unaffected while M1 is standstill and accelerated. These experiments demonstrate that the proposed scheme is capable of independent control of two split-phase motors.

The effectiveness of AUX VSI (capacitive filter) modulation for the proposed parallel connected topology is tested and shown in Fig. 12(a). The MAIN VSI is modulated with $V^*_{\alpha\beta}$ reference voltages while keeping $V^*_{z_1 z_2} = 0$; hence, M1 is operating at a constant speed of 900 r/min and M2 is at standstill condition. Initially AUX VSI-1 is modulated, whereas AUX VSI-2 is not switched. It can be noted from the figure that M1 is running and drawing a constant steady-state current, but M2 is standstill but still drawing currents at the same frequency as M1. The currents through M2 are basically the harmonic currents ($\alpha - \beta$ current), which flow because of the absence of back EMF. In this case, and at the same time, there are no suppressing voltages generated by the AUX VSI-2 during this period.

At time t_1, AUX VSI-2 is modulated to produce the exact $V_{\alpha\beta}$ voltage at the inverter output to suppress the $\alpha - \beta$ harmonic currents through M2. It can be noted that the M2 currents decay to zero as shown in Fig. 12(a).2. It can also be noted that the phase current envelope of M1 remains constant throughout as shown in Fig. 12(a).1. The current of MAIN VSI is (sum of M1 and M2 currents) shown in (a).3. Initially the dc link of AUX VSI-2 (V_{dc2}) was nearly zero as there were no pulses given to the IGBT switches, but finally charged to its steady-state value after AUX VSI-2 starts switching at t_1. This proves the effectiveness of the capacitor-fed auxiliary inverters.

The proposed topology provides a inherent voltage balancing capability for the dc links of AUX VSIs. Fig. 12(b).1 and 2 show the dc link of AUX VSI-1 (V_{dc1}) and AUX VSI-2 (V_{dc2}) which build up from zero volts to the steady-state nominal voltage of 100 V, during start-up and (b).3 shows the dc link of MAIN VSI ($V_{\mathrm{dc}} = 200$ V), which is fed from a three-phase bridge rectifier. The MAIN VSI current envelope is shown in (b).4 during start-up transients.

From the presented results, it can be observed that for all operating conditions, the phase currents of one motor are unaffected during the transient conditions of other motor, which proves that the motor currents are independent and decoupled from each other. In all operating conditions, the dc link of the AUX VSIs is inherently regulated (without any voltage balancing circuit or control scheme) as shown in plots. The AUX VSIs block the flow of fundamental and harmonic currents of M1 through M2 and vice versa. Thus, the phase currents of individual motor become sinusoidal and void of harmonics. A completely decoupled operation can be achieved in this parallel connected topology and both the motors can be operated at their full rated power without derating of the motors.

V. Conclusion

In this paper, a parallel connected multimotor drive scheme is proposed for the first time using a single power source and color red capacitor-fed auxiliary inverters. As opposed to the existing multimachine schemes, the proposed scheme can be operated up-to full power rating of the machines simultaneously without the requirement for machine derating. In addition, the switching frequency of the main inverter can be reduced due to the AUX VSIs, thereby eliminating the need for bulky inductive filters. Furthermore, three modulation schemes were also proposed for the scheme namely, sine triangle and two types of space-vector PWM methods. Detailed experimental results were presented to validate the decoupled operation of the proposed system.

From the experimental results, it can be concluded that it is possible to operate both the motors in completely decoupled manner for all conditions including transients. The dc link of the AUX VSIs remains stable for both steady state and transients, and does not require any precharging and voltage balancing circuits or control techniques due to its inherent balancing capability. With advantages such as low switching frequency, decoupled and coordinated control while being fed from a single VSI, reduced power ratings of auxiliary inverters, inherent voltage balancing capability for the dc links of AUX VSIs, and full power-range operation of the machines, the proposed topology can be considered as a viable scheme for multimotor industrial drive applications.

References

[1] L. Parsa, "On advantages of multi-phase machines," in *Proc. 31st Annu. Conf. IEEE Ind. Electron. Soc.*, 2005, p. 6.

[2] T. M. Jahns, "Improved reliability in solid-state ac drives by means of multiple independent phase drive units," *IEEE Trans. Ind. Appl.*, vol. IA-16, no. 3, pp. 321–331, May 1980.

[3] K. Gopakumar, V. Ranganthan, and S. Bhat, "Split-phase induction motor operation from PWM voltage source inverter," *IEEE Trans. Ind. Appl.*, vol. 29, no. 5, pp. 927–932, Sep./Oct. 1993.
[4] K. Gopakumar, S. Sathiakumar, S. Biswas, and J. Vithayathil, "Modified current source inverter fed induction motor drive with reduced torque pulsations," *IEE Proc. B (Elect. Power Appl.)*, vol. 131, no. 4, pp. 159–164, Jul. 1984.
[5] M. A. Abbas, R. Christen, and T. M. Jahns, "Six-phase voltage source inverter driven induction motor," *IEEE Trans. Ind. Appl.*, vol. IA-20, no. 5, pp. 1251–1259, Sep. 1984.
[6] Y. Zhao and T. A. Lipo, "Space vector PWM control of dual three-phase induction machine using vector space decomposition," *IEEE Trans. Ind. Appl.*, vol. 31, no. 5, pp. 1100–1109, Sep./Oct. 1995.
[7] E. A. Klingshirn, "Harmonic filters for six-phase and other multiphase motors on voltage source inverters," *IEEE Trans. Ind. Appl.*, vol. IA-21, no. 3, pp. 588–594, May 1985.
[8] N. A. Azeez, K. Gopakumar, J. Mathew, and C. Cecati, "A harmonic suppression scheme for open-end winding split-phase IM drive using capacitive filters for the full speed range," *IEEE Trans. Ind. Electron.*, vol. 61, no. 10, pp. 5213–5221, Oct. 2014.
[9] K. Gopakumar, V. Ranganathan, and S. Bhat, "An efficient PWM technique for split phase induction motor operation using dual voltage source inverters," in *Proc. Ind. Appl. Soc. Annu. Meeting*, 1993, pp. 582–587.
[10] E. Levi, "Advances in converter control and innovative exploitation of additional degrees of freedom for multiphase machines," *IEEE Trans. Ind. Electron.*, vol. 63, no. 1, pp. 433–448, Jan. 2016.
[11] E. Levi, M. Jones, S. N. Vukosavic, and H. A. Toliyat, "A novel concept of a multiphase, multimotor vector controlled drive system supplied from a single voltage source inverter," *IEEE Trans. Power Electron.*, vol. 19, no. 2, pp. 320–335, Mar. 2004.
[12] T. Lipo, *A Cartesian Vector Approach to Reference Frame Theory of AC Machines*. Madison, WI, USA: Dept. Elect. Comput. Eng., Univ. Wisconsin-Madison, 1984.
[13] S. Gataric, "A polyphase cartesian vector approach to control of polyphase ac machines," in *Proc. Ind. Appl. Conf. Rec.*, 2000, vol. 3, pp. 1648–1654.
[14] K. K. Mohapatra, R. Kanchan, M. Baiju, P. Tekwani, and K. Gopakumar, "Independent field-oriented control of two split-phase induction motors from a single six-phase inverter," *IEEE Trans. Ind. Electron.*, vol. 52, no. 5, pp. 1372–1382, Oct. 2005.
[15] M. Jones, S. Vukosavic, and E. Levi, "Independent vector control of a six-phase series-connected two-motor drive," in *Proc. 2nd Int. Conf. Power Electron., Mach. Drives*, 2004, vol. 2, pp. 879–884.
[16] E. Levi, M. Jones, and S. Vukosavic, "Even-phase multi-motor vector controlled drive with single inverter supply and series connection of stator windings," *IEE Proc.-Elect. Power Appl.*, vol. 150, no. 5, pp. 580–590, Sep. 2003.
[17] E. Levi, A. Iqbal, S. Vukosavic, and H. Toliyat, "Modeling and control of a five-phase series-connected two-motor drive," in *Proc. 29th Annu. Conf. Ind. Electron. Soc.*, 2003, vol. 1, pp. 208–213.
[18] M. Jones, S. N. Vukosavic, and E. Levi, "Parallel-connected multiphase multidrive systems with single inverter supply," *IEEE Trans. Ind. Electron.*, vol. 56, no. 6, pp. 2047–2057, Jun. 2009.
[19] S. K Dash, S. Ranjith, and K. R. Sudharshan, "Decoupled control of dual-split-phase IMs for full power range using capacitive filters," in *Proc. IEEE Int. Conf. Power Electron., Drives Energy Syst.*, 2018.
[20] S. K Dash and K. R. Sudharshan, "Space vector PWM techniques for parallel connected dual-split-phase IMs for full power range using capacitive filters," in *Proc. 8th India Int. Conf. Power Electron.*, 2018.
[21] A. Iqbal and E. Levi, "Space vector PWM for a five-phase VSI supplying two five-phase series-connected machines," in *Proc. 12th Int. Power Electron. Motion Control Conf.*, 2006, pp. 222–227.

Sagar Kumar Dash (S'18) received the M.Tech. degree in power electronics from Indian Institute of Space Science and Technology, Thiruvananthapuram, India, in 2018. He is currently working toward the Ph.D. degree at Indian Institute of Technology Kharagpur, Kharagpur, India.

His research interests include multiphase machines, motor drives and control.

R. Sudharshan Kaarthik (M'12) received the B.Tech. degree in electrical engineering from the National Institute of Technology, Rourkela, India, in 2010, and the M.Tech. degree in electronics design and technology and the Ph.D. degree in power electronics from the Indian Institute of Science, Bengaluru, India, in 2012 and 2015, respectively.

He was a Postdoctoral Fellow with Concordia University, Montreal, QC, Canada, till 2017. He is currently appointed as an Assistant Professor with the Department of Avionics, Indian Institute of Space Science and Technology, Thiruvananthapuram, India. His research interests include multilevel inverters and motor drives.